Optoelectronic properties of thick SiGe layers grown as small mesas by low pressure chemical vapor deposition

T. Stoica[a] and L. Vescan
Institut für Schichten und Grenzflächen (ISG), Forschungszentrum Jülich GmbH, D-52425 Jülich, Germany

(Received 18 November 2002; accepted 20 January 2003)

Arrays of $Si_{0.80}Ge_{0.20}/Si(001)$ square mesas were epitaxially grown by low pressure chemical vapor deposition to optimize the light emission in the near infrared range. To study the influence of mesa size on light emission the current–voltage characteristics, the spectral photocurrent, and the electroluminescence of *p-i-n* structures were measured. While the plastic relaxation has a strong influence on the electroluminescence spectra, the current–voltage characteristics are only slightly changed. At low temperatures, a tunneling current was observed and its possible location is discussed. Due to the high SiGe thickness, both the contributions of the no-phonon and transversal optical phonon-assisted transitions to the photocurrent spectra could be observed. Direct evidence of the higher band gap of relaxed SiGe was obtained from electroluminescence studies. © *2003 American Institute of Physics.* [DOI: 10.1063/1.1559636]

I. INTRODUCTION

The optoelectronics today is based mainly on III–V semiconductors. SiGe optoelectronic devices are currently investigated as well, because of the advantages offered by this material: the possibility of integrating the optical and high speed electronic functions on a Si substrate. Adding Ge to Si increases the absorption (essential for detection) and the refractive index (necessary for light guiding). The lattice mismatch between SiGe alloys and Si substrate is partly a problem due to the plastic relaxation, but on the other hand the strain induced band gap lowering allows emission at the near infrared wavelength range. The only real problem is the indirect band gap which poses obstacles for light emission. Even so, it was demonstrated that infrared light with a wavelength longer than 1.2 μm can be guided, modulated, switched, detected, and even emitted from SiGe.[1,2]

However, even if in the last years the external quantum efficiency of SiGe-based light emitting diodes (LEDs) could be increased by orders of magnitude,[3] the present values are too low for any application. One way to increase quantum efficiency is to optimize the design of the diode structure, to reduce the recombination outside SiGe layer and to optimize the SiGe thickness.[4] The room temperature efficiency of the electroluminescence (EL) increases with SiGe thickness, as was demonstrated earlier for fully strained $Si_{0.80}Ge_{0.20}$.[3,4] The selective growth on small area can be used for increasing the critical thickness of SiGe layer. Therefore, for further improving the efficiency of light emission studies of carrier injection and recombination effects in small SiGe mesas are necessary.

In this article mesa size effects on EL and current–voltage ($I-V$) characteristics of different diodes with thick SiGe layers have been investigated. The plastic relaxation was studied by EL and phototoluminescence (PL). The $I-V$ curves show at low temperatures the influence of mesa facets and of tunneling current. The spectral photocurrent (PC) data are compared with the EL results. At low temperature the contribution of no-phonon (NP) and transversal optical (TO) phonon-assisted transitions are well resolved by the spectral PC. Previous studies at room temperature for SiGe diodes with different Ge concentrations have shown only the contributions of phonon-assisted optical transitions with absorption and emission of phonons.[5] Direct evidence of the band gap increase due to strain relief by plastic relaxation and of the NP absorption transitions in SiGe layers is obtained by EL and PC measurements, respectively. The low measurement temperature and the high thickness of the strained SiGe layers allowed the observation of NP absorption transitions.

II. EXPERIMENTAL DETAILS

The selective epitaxial growth was carried out by low pressure chemical vapor deposition at 700 °C with $R_{SiGe} = 14\ \text{nm min}^{-1}$, flow $(SiCl_2H_2) = 10$ sccm, flow $(GeH_4) = 1$ sccm, flow $(H_2) = 200$ sccm, and $p_{tot} = 0.1$ Torr. n^+ Si(001) wafers ($N_D \sim 10^{19}\ \text{cm}^{-3}$) were oxidized and patterned with square holes with sizes from 4 μm to 1 mm. *p-i-n* diodes in the form of mesas were grown with the layer sequence n^+np^+: (1) n^+-Si buffer, (2) *n*-Si buffer, (3) n-$Si_{1-x}Ge_x$ ($x = 0.20–0.28$, thickness: 70–450 nm), (4) n-$Si_{1-x}Ge_x$ ($x = 0.02$; 20–60 nm), and (5) boron doped $Si_{1-x}Ge_x$ ($x = 0.02$, thickness ~ 100 nm). The ohmic front and bottom contacts were evaporated Al/Au (or ZnO) and AuSb, respectively. Other deposition and diode fabrication details are given in Refs. 4, 6, and 7. The samples investigated are described in Table I. The *n*-type doping represents the phosphorus concentration measured by secondary ion mass spectroscopy (SIMS).

[a]Author to whom correspondence should be addressed; electronic mail: t.stoica@fz-juelich.de

TABLE I. Data of $Si_{1-x}Ge_x$/Si LED structures.

Sample No.	Buffer thickness (nm)	Buffer doping (cm^{-3})	Ge content x	SiGe thickness (nm)	SiGe doping (cm^{-3})	Spacer thickness (nm)	Top contact
1597	230	$\sim 2\times10^{17}$	0	0	—	—	ZnO
1296	260	8×10^{17}	0.21	260	1×10^{18}	30	Al/Au
1108	600	3×10^{16}	0.20	370	3×10^{16}	21	Al/Au
1687	580	8×10^{17}	0.21	445	1×10^{18}	24	Zno

III. RESULTS AND DISCUSSIONS

A. The influence of plastic relaxation on the spectral distribution of PL and EL

By selective epitaxy on patterned wafers fully strained SiGe layers can be grown with a thickness much higher than the critical value for misfit dislocation (MD) formation on large area. The reduction of MD density on small mesas comprises two aspects. One is related to the equilibrium elastic relaxation of strained SiGe/Si mesas. This effect becomes important only for small sizes on the order of 1 μm and below. Another aspect is related to the metastable state of the strained layers on relatively large mesas (lateral size up to few 100 μm for $x=0.10-0.20$ and growth temperature of 700 °C).[8–12] The metastable state is due to the relative long specific times of the extrinsic nucleation of MDs at point defects and the self-multiplication process.[13]

Fully strained $Si_{0.80}Ge_{0.20}$ diodes were obtained up to a thickness of 445 nm for mesas with size of 50 μm or smaller, using selective epitaxy. This thickness is 30 times higher than the critical value given by the equilibrium theory and is 6 times higher than the experimental value for metastable state of the SiGe layers on large areas. In Fig. 1 the theoretical curve of the critical thickness in dependence on Ge concentration is shown in comparison with experimental data on metastable strained SiGe layers deposited by selective epitaxial growth (SEG) on large area and in patterns with different sizes (equilibrium curve—Matthews and Blakeslee theory;[14] dotted line-experimental metastable on large area;[15] points are for different sizes of the mesas: 10 and 300 μm;[16] strained diodes with 50, 200, and 24 μm—this article). The MD density function of the deposition area have been analyzed within previous articles.[11–13]

The plastic relaxation has a major effect on the electrical and photoelectrical properties of SiGe structures. The presence of dislocations may quench all other radiative recombination paths. An illustration of the mesa-size dependence of the plastic relaxation on PL and EL is shown in Fig. 2. The PL from large area sample in Fig. 2(a) shows high emission due to the dislocation related defects within the spectral range of 750–950 meV and only a weak contribution at low temperature from the Si substrate and the SiGe layer. The dislocation peaks are the well known $D1$ and $D2$ peaks,[17] while the broad peak at higher energy (T-band) indicates a high density of isoelectronic centers in the SiGe layer which occur during the relaxation process.[18] In contrast to the large

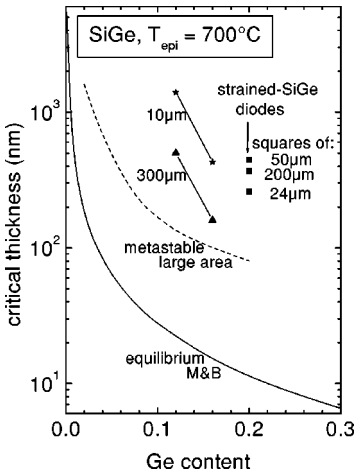

FIG. 1. Critical thickness for SiGe/Si(001) in function of Ge concentration: solid line is the prediction of Matthews and Blakeslee equilibrium theory (Ref. 14); dotted line is the experimental metastable curve obtained on large area for 700 °C (Ref. 15); other points are for strained SiGe grown by SEG on different square mesas (10 and 300 μm—Ref. 16; strained diodes this article—50 μm No. 1687, 200 μm No. 1108, and 24 μm No. 1296).

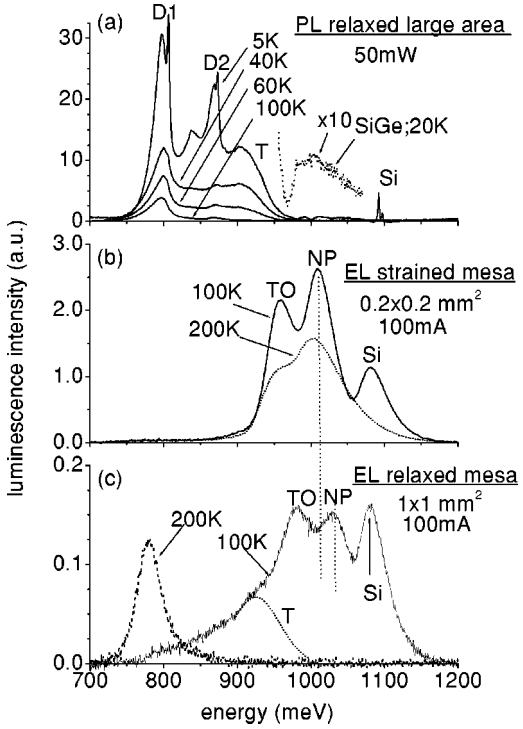

FIG. 2. Influence of plastic relaxation on the luminescence spectra of a 370 nm thick $Si_{0.80}Ge_{0.20}$ sample (No. 1108): and (a) PL of a plastically relaxed large area part, (b) EL of a strained 0.2 mm square mesa, and (c) EL of a relaxed 1 mm mesa. All three graphs have the same arbitrary units, thus a comparison of the intensities is possible.

TABLE II. TO and NP peak energies for various growth area (sample No. 1108).

PL/EL	Sample area (mm^2)	Injection intensity	T (K)	E_{TO} (meV)	E_{NP} (meV)	Strain state
PL	large area	50 mW	5	993	—	relaxed
EL	1×1	100 mA	100	979	1037	relaxed
EL	1×1	60 mA	100	973	1029	relaxed
EL	0.2×0.2	100 mA	25	954	1011	strained
EL	0.2×0.2	100 mA	100	960	1010	strained
EL	0.2×0.2	50 mA	25	953	1009	strained
EL	0.2×0.2	50 mA	100	958	1012	strained

area emission, the EL of 0.2 mm mesa diodes shows no contribution from dislocations [Fig. 2(b)], implying no plastic relaxation of the mesa. Beside the NP and TO peaks from the strained SiGe, emission from Si can be seen up to 100 K. This peak is correlated to the TO emission in doped Si regions.

Larger diodes ($1\times1\ mm^2$) on the same wafer are plastically relaxed, thus at 200 K only MD-related emission appears [Fig. 2(c)]. At 100 K most of the injected carriers remain captured in the SiGe layer, thus recombining radiatively. However, the emission is much weaker than in nonrelaxed diodes. One reason can be the strong recombination at deep traps related to the isoelectronic centers mentioned above and seen as a shoulder (T) in Fig. 2(c). The defects related to MDs give at this low temperature only a broad contribution at the low energy side of the TO–SiGe band-to-band transition. By increasing the temperature, the carriers from higher energetic states of SiGe and Si are thermally excited and captured on the lower lying energy states of dislocation regions.

It is worth mentioning that the EL measurement allowed us to observe the increase of the energy gap due to strain relaxation. Thus, comparing the EL spectra of Fig. 2(b) (not relaxed) with Fig. 2(c) (relaxed) one can see that the energy gap of $Si_{0.80}Ge_{0.20}$ increases, and the NP peak shifts from ~1009 meV (strained) to ~1037 meV (relaxed) (see also Table II). The shift of 28 meV corresponds to a strain relaxation of 35% in the 1 mm SiGe mesas.

The competition of the different recombination paths (Si, SiGe, and dislocation related defects) is in fact more complicated than described here due to the different dependencies of the recombination mechanims on injected current and temperature. For instance, by increasing the temperature the Si emission can be reduced if recombination takes place only in the SiGe layer, but can increase again at higher temperature due to the thermal emission of the carriers from SiGe. Moreover, the contribution to the emission from Si and dislocation regions increases relatively to that of SiGe layer itself, by increasing the injection current.

B. Current–voltage characteristics

Figure 3 displays room temperature $I-V$ characteristics of diodes deposited in the same run for various mesa areas and a SiGe thickness of 260 nm. The mesa size was varied from 4 to 500 μm. At high forward voltage the current is limited by series resistances. A thermal annealing of the Al/Au contacts at 350 °C is necessary to reduce the contact series resistance [the 4 and 24 μm diodes were annealed and have a smaller series resistance as compared to the unannealed diodes (50 and 500 μm)].

One feature of the $I-V$ characteristics for small forward biases is that the current is proportional to the area over 7 orders of magnitude for all sizes. This implies no contribution of leakage current at the diode periphery. However, the smaller diodes (size of 4 μm) have a ten times higher current density than the larger diodes, although the ideality factor remains almost the same (1.70–1.73) independent on the leakage current. This increase of current density in forward and reverse biases for small mesas can be explained by a higher current density across the facets than through the (001) top of the mesa. This is due to the fact that the growth rate on facets is smaller than on the (001) mesa top, resulting in a thinner spacer between the SiGe layer and p^+ contact (from 30 to 15 nm for this sample). Therefore, the current density is increased, as shown previously by numerical simulations.[7] Because the 4 μm diodes have a facet area of the same order of magnitude as the total area, the total current density is sensibly increased.

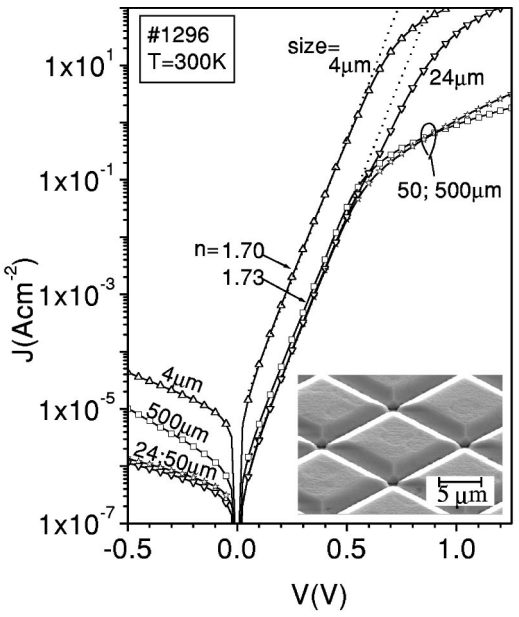

FIG. 3. $I-V$ characteristics of mesa diodes with different deposition areas. The 4 and 24 μm diodes were annealed, while the 50 and 500 μm diodes are unannealed. The inset shows a SEM picture of an array of diodes connected in paralel with transparent conducting ZnO contacts.

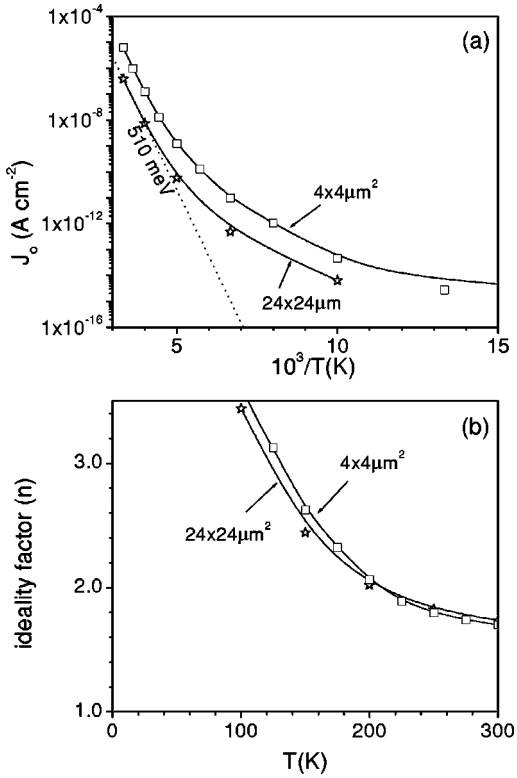

FIG. 4. Temperature dependence of (a) saturation current J_o and (b) ideality factor n for diodes deposited in one run but with different mesa areas.

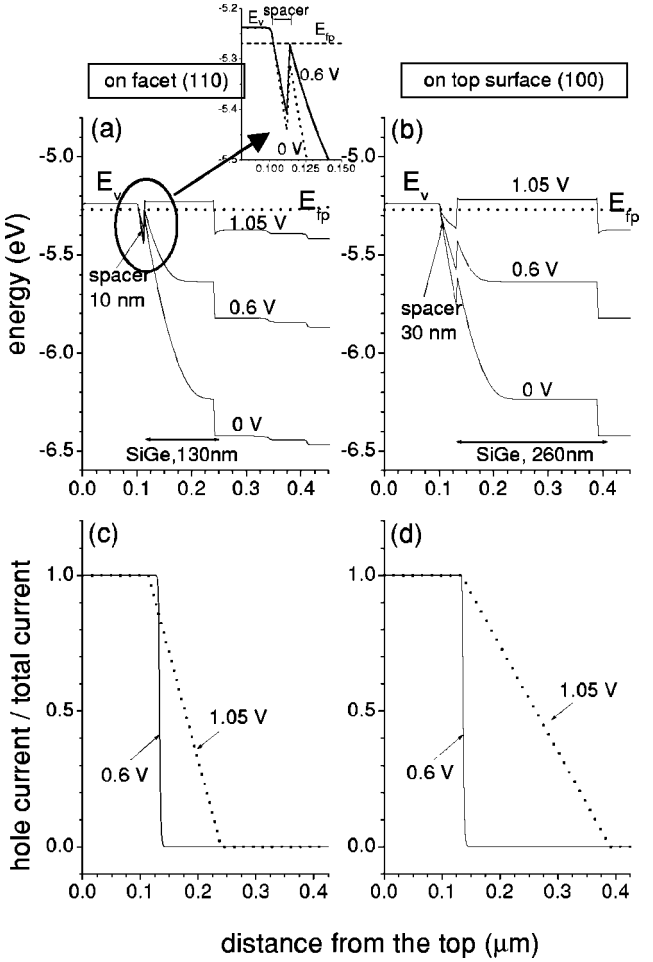

FIG. 5. Simulation of the depth dependence at 100 K and different bias voltages for a diode of epitaxy No. 1296: (a) and (b) valence band E_v and hole quasi-Fermi level band E_{fp}; (c) and (d) hole current profile. The parameters of the facet regions for the curves in (a) and (c): spacer $=10$ nm; thickness of SiGe$=130$ nm. The same doping levels are for facets as well as the top regions (the parameters for the top regions are given in Table. I).

The $I-V$ curves were measured at different temperatures within the range 20–300 K. The linear region of the logarithmic representation can be well fitted for all temperatures with the expression $J \approx J_0 \exp(eV/nkT)$ used for a pn junction with diffusion and recombination currents (e is electron charge, k is Boltzmann constant, and T is absolute temperature).

The temperature behavior of the $I-V$ curves is independent of mesa area (with or without dominant facet current contribution). Figure 4 displays for the 4 and 24 μm diodes the temperature dependencies of the current extrapolated to zero voltage J_0 and the ideality factor n. In the range 200–300 K, $n<2$ and the J_0 has an exponential temperature dependence with an activation energy of ~ 510 meV. This value is about the half the energy gap, as expected for recombination-limited forward current. Below 200 K, n increases rapidly while the energy nkT decreases toward a finite value of ~ 28 meV at low temperatures.

The weak temperature dependence of the $I-V$ curves below 100 K indicates a strong contribution of tunneling current. We performed simulation of the band diagram of a p-i-n diode using the SIMWIN program.[19] Only drift-diffusion and recombination equations have been considered. Even if the quantum process of tunneling has not been simulated, the band diagram illustrates the possible location of the tunneling process.

The simulation has been performed for the mesa edge region assuming (110) facets and the top surface (100). The facet regions correspond to thinner epitaxial layers due to the smaller growth rate. The parameters of the simulated structure correspond to the deposition No. 1296 (Table I). The depth dependencies of the valence band extrema E_v of the facet and the top (001) regions are shown in Figs. 5(a) and 5(b) for 100K and three values of the bias (0, 0.6, and 1.05 V). The quasi Fermi-level for holes ($E_{\rm fp}$) remains almost constant in the plotted range. The corresponding hole current profile is represented in Figs. 5(c) and 5(d) as the ratio of the hole current to the total current. This hole current profile gives information about the recombination regions, i.e., where the current drops to zero. For small forward biases, due to the high electric field at the $p-i$ junction, the valence band at the top Si/SiGe interface has a well of triangular form. This well remains below $E_{\rm fp}$ for voltages below 0.5 V. For 0.5–0.6 V the valence band spike comes very close to the $E_{\rm fp}$ in the case of the thinner spacer (10 nm) as can be seen in Fig. 5(a) and in the enlarged picture of the inset of this figure. In this case the holes at the left side of the spacer ''see'' states at the same energy in the well, thus tunneling takes place. At small voltages, the electron-hole recombination occurs in a very narrow space near to the spike of the valence band, as can be seen from the diagram of the hole

current in Fig. 5(c) for voltage of 0.6 V. The hole current drops very abruptly to zero in the well region. We can conclude that for thin spacers and low temperature the current through the p^+-i junction at small forward voltages is limited by the region of the spacer and valence band spike. Thus, holes which tunnel from p^+ region to the triangular valley at the top Si/SiGe interface give the major contribution to the current. For thicker spacer of 30 nm [Fig. 5(b)] the spike in valence band approaches E_{fp} only for high injection levels. Therefore, at low temperature and low forward voltages the tunneling current through facets may dominate the current.

At higher forward voltage, the valence band in the whole SiGe becomes approaches the quasi Fermi-level as can be seen in Figs. 5(a) and 5(b) the curves at 1.05 V. A high hole density with a nearly uniform spatial distribution is obtained in this case and the recombination extends to the whole SiGe region [Figs. 5(c) and 5(d)]. Our EL investigations are limited to this diode regime (biases$>$1 V).

It is worth to mention that at low temperature the $I-V$ curves show small oscillations of the logarithmic slope of the forward current. These oscillations may be explained by the energy quantization in the spike region of the valence band (see Fig. 5).

We have seen in Sec. III A that the plastic relaxation has a strong influence on the PL and the EL spectra. The strain relaxation influences to some extend also the $I-V$ characteristics. A SiGe thickness of 260 nm is well above the critical thickness for plastic relaxation. Therefore, large diodes of 500 μm size are relaxed (see Sec. III A). While the plastic relaxation influences the forward current insignificantly, the reverse current is increased by the presence of MDs (a factor of 10 for the 500 μm diodes, see Fig. 3). For this type of mesa diode, the forward current increases with voltage much faster and covers the leakage current due to MD regions. To understand the relative weak influence of the MDs on the $I-V$ curves we have to keep in mind that the growth procedure is local growth of small mesas by SEG. In this case, most of the MDs extend from one of the side of the mesa diode to the other. Only few threading dislocations (TDs), i.e., those at the ends of MDs exist in the diode bulk. Even if the mesas are plastically relaxed the MD density is much lower than on extended areas.[11] On the contrary, the diodes made on unpatterned areas have a high density of TDs statistically distributed in the diode. The TDs which cross the diode junction increase the current much more than MDs do, which lie buried in the bottom SiGe/Si interface plane, thus being parallel to the junction. Therefore, the current for diodes obtained by SEG is less increased by plastic relaxation than expected for diodes obtained by deposition on extended areas. While for the $I-V$ curves of selectively grown diodes the dislocations have little influence, significant changes of the light emission are observed because of the carrier recombination in the dislocation region, as seen in Sec. III A.

There also is an influence of the SiGe thickness on the current through the diode. The current and ideality factor increase by increasing the SiGe thickness due to the higher contribution of the generation-recombination processes. For example, an increase of the SiGe thickness by a factor of 2 (from 260 to 445 nm) increases the forward current by a factor of 8 for strained diodes.

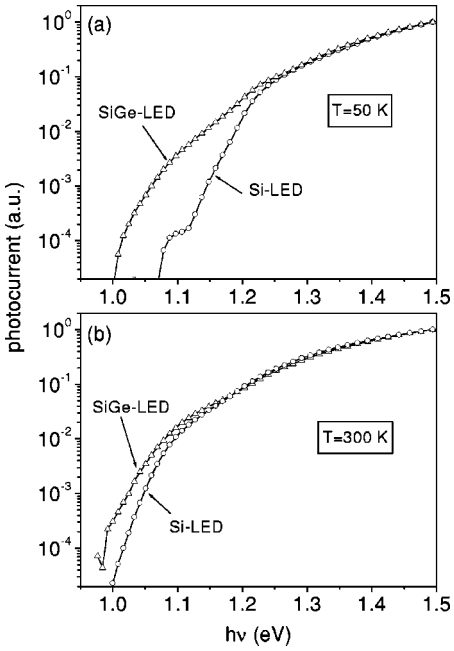

FIG. 6. Comparison of spectral photocurrent for SiGe (No. 1296) and Si (No. 1597) diodes at: (a) 50 K; and (b) 300 K.

To conclude, $I-V$ measurements have provided useful information about the carrier injection processes in SiGe diodes and support the assumption for EL at high current levels that the injected holes are uniformly distributed within the SiGe layer.

C. Photocurrent spectroscopy

The photocurrent measurements on EL diodes usually provide information about the optical transitions. In particular the optical energy gap and the phonon energies can be evaluated. We have performed spectral photocurrent measurements on SiGe diodes comparatively with pure Si diodes. The short-circuit current of the diodes was measured using a grating monochromator. The photon energy was varied in the range 0.9–1.55 eV and the temperature in the range 50–300 K. The light intensity was calibrated using a Ge detector with known sensitivity curve. The spectral photocurrent efficiency $J_{\mathrm{PC}}(h\nu)$ was obtained as the ratio of the measured current and the photon number. Due to the uncertainty of the absolute intensity of the incident light, we consider here the J_{PC} in arbitrary units, as the absolute value has no consequences for the analysis in this section.

The SiGe diodes show a photocurrent signal due to carriers generated in the SiGe layer, but also from Si regions. To identify univoquely the SiGe contribution we have fabricated pure Si diodes, too. The spectral photocurrent curves $J_{\mathrm{PC}}(h\nu)$ are shown in a logarithmic scale in Fig. 6 for SiGe and Si diodes at 50 and 300 K. For an easier comparison, the spectra were normalized to unity at the photon energy of 1.5 eV. At low temperature and below 1.15 eV there is a large difference between the SiGe and Si spectra. At room temperature, this difference is smaller.

From the low temperature spectra the optical energy gap can be evaluated. The photogeneration of the carriers has be taken proportional to the absorption coefficient. The classical formula for the absorption coefficient of phonon assisted indirect transitions is given by[20]

$$\alpha(h\nu)=A\frac{(h\nu-E_g\pm E_{\text{phon}})^2}{h\nu}f_{\text{ct}}(E_{\text{phon}},T), \tag{1}$$

where $f_{\text{ct}}=1/[\exp(\pm E_{\text{phon}}/kT)\mp 1]$; + or − sign is for phonon absorption or emission transitions, E_{phon} is phonon energy, and E_g is optical energy gap. The last factor in Eq. (1) is related to the phonon occupation function. In a plot of $(\alpha h\nu)^{1/2}$ a linear dependence on $h\nu$ is obtained with extrapolation to zero at $E_g\mp E_{\text{phon}}$. In SiGe the most probable indirect transitions are for transversal optical phonons, thus $E_{\text{phon}}=E_{\text{TO}}$. For NP transitions involving disorder, such as alloy disorder in SiGe, the spectral distribution of absorption coefficient is similar to that in Eq. (1). For this NP absorption $E_{\text{phon}}=0$ and $f_{\text{ct}}=1$ must be taken.

At low temperature, the near band gap absorption in SiGe is dominated by emission of TO phonons and by NP processes. These transitions were not simultaneously evidenced in previous articles.[5,21] The present experimental data allowed us to put into evidence both NP and TO assisted transitions in the spectral photocurrent due to the much thicker SiGe layers. Assuming $J_{\text{PC}}(h\nu)\sim\alpha(h\nu)$, a sum of the NP and TO expressions for the absorption coefficient [Eq. (1)] was fitted to the experimental data of the spectral photocurrent. The fitting curves of NP and TO emission transition are shown in Fig. 7(a) in comparison with the experimental curves at 50 K for SiGe and Si diodes. An EL spectrum measured on the same SiGe sample at low current and low temperature is also included. The optical gap and transversal optical phonon energies were found with the values $E_g(\text{SiGe})=993$ meV and $E_{\text{TO}}=55$ meV, respectively. The energy gap is lower than the expected value of 1002–1007 meV for $x=0.20$.[22–25] The smaller gap value found from our spectral photocurrent data can be explained by a doping-induced energy gap narrowing, as the corresponding sample has a phosphorus doping of $\sim 10^{18}$ cm^{-3} (Table I).

As discussed above, the errors in energy gap evaluation are higher at higher temperatures due to the superposition of spectra of many absorption processes in SiGe as well in Si regions (Fig. 6). However, the temperature dependence of the optical gap was evaluated using the spectral photocurrent data for the SiGe sample at different temperatures. The results are shown in Fig. 8 in comparison with values obtained from EL investigations. One can see that the gap energy evaluated from the spectral photocurrent is higher than that evaluated from EL. This can be explained by electron hole plasma effects observed in EL experiments.[26]

The phonon energy $E_{\text{TO}}=55$ meV obtained at 50 K from PC is in good agreement with the value 55–56 meV obtained from fitting the experimental EL spectra to the electron hole plasma (EHP) model.[26] The optical gap value [Fig. 7(a)] is higher than the value of 982 meV found from EL analysis at lower current injection and low temperature (Fig. 8). The difference of about 10 meV can be explained by the band filling effect (Moss–Burstein effect) and by higher EHP density in EL experiments which corresponds to a smaller renormalized gap.

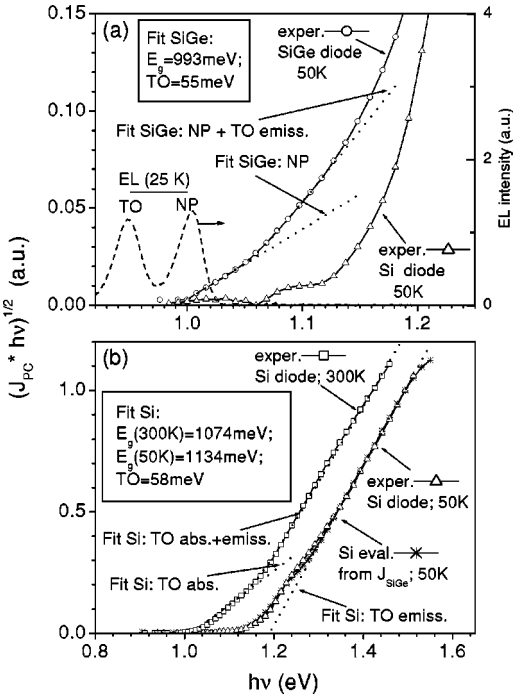

FIG. 7. Square root representation of spectral photocurrent: (a) fitting curves of NP and TO phonon emission optical transitions (dotted curves) and experimental data of SiGe (No. 1296) and Si (No. 1597) diodes at 50 K. The EL spectrum of the same diode at 25 K and 10 mA is also shown; (b) evaluated Si contribution to photocurrent of SiGe diode at 50 K in comparison with data from the Si diodes at 50 and 300 K (dotted curves are fitting curves for TO phonon absorption and emission processes in Si regions).

By subtracting the SiGe(NP+TO) generation part [dotted curve in Fig. 7(a)] from the total photocurrent, the Si contribution could be estimated. This Si part of the spectral

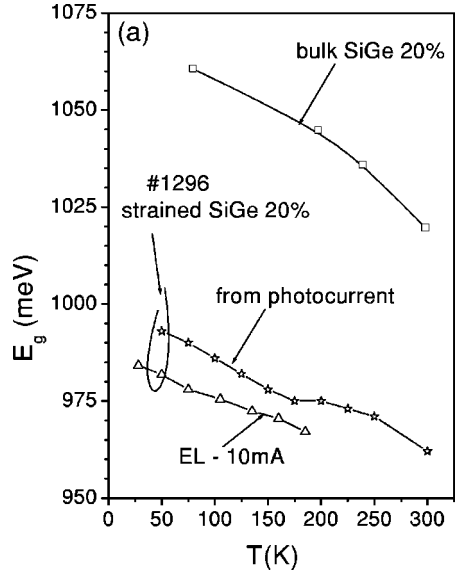

FIG. 8. Temperature dependence of the optical gap deduced from spectral photocurrent in comparison with renormalized band gap deduced by line shape analysis of EL spectra at low injection current 10 mA (Ref. 26) and the band-gap of bulk SiGe with $x=0.20$ (Ref. 27, p. 127).

photocurrent in SiGe diode at 50 K is shown in Fig. 7(b) in comparison with the measured spectrum of the pure Si diode. A good agreement is obtained. In addition, in Fig. 7(b) the photocurrent of the Si diode at 300 K is displayed. The curves for measured Si photocurrent are similar to the earlier published data on Si (see for example Ref. 20). At 300 K, the two contributions of TO absorption and emission processes could be fitted with the sum of corresponding expressions of Eq. (1) with $E_g = 1074$ meV and $E_{TO} = 58$ meV. At 50 K, we find $E_g(\mathrm{Si}) = 1134$ meV from the TO emission curve in Fig. 7(b). A band gap narrowing of 34–50 meV could be evaluated, which corresponds to a donor density in the range 10^{17}–10^{18} cm^{-3},[28] in good agreement with SIMS data for sample Nos. 1296 and 1597 in Table I.

IV. CONCLUSIONS

The photocurrent spectra on diodes with thick SiGe layers give reliable information on the near band gap optical transitions of the TO and NP processes at low temperatures. The investigations are useful for the knowledge of the injection and recombination processes in thick SiGe for optimizing the light emission of the LED structures.

The thickness of $Si_{0.80}Ge_{0.20}$ fully strained layers could increased more than ten times the critical thickness for plastic relaxation by using selective epitaxial growth of small square mesas of 4–100 μm width. The misfit dislocations formed on larger deposited areas influence strongly the emission spectra, whereas only weak changes in the $I-V$ curves occur. This is due to the extension of the dislocations up to the mesa edges in the case of selective epitaxy, leaving the diode volume with a small density of threading dislocations. The blueshift of the electroluminescence peak due to plastic relaxation is shown by comparing spectra of relaxed and fully strained SiGe diodes.

The $I-V$ characteristics of SiGe diodes have ideality factors of 1.7–2 above 200 K. At low temperatures the tunneling current dominates the $I-V$ characteristics. Based on the simulation of band structure the possible location of the tunneling phenomenon was suggested. The influence of the facets for small mesa diodes was revealed.

The contributions of no-phonon and TO phonon-assisted transitions are well resolved at low temperature in photocurent spectra of diodes with fully strained thick SiGe. The temperature dependence of the optical gap is in agreement with results of EL analysis and data from literature.

ACKNOWLEDGMENTS

The authors are grateful to Bernd Holländer for the RBS studies, to Andreas Mück for the SIMS studies and to Hilde Siekmann for the ZnO deposition.

[1] S. Pogossian and A. Vonsovici, Recent Res. Devel. Optics **1**, 19 (2001).
[2] G. Masini, L. Colace, and G. Assanto, Mater. Sci. Eng., B **89**, 2 (2002).
[3] L. Vescan and T. Stoica, Proc. SPIE **3630**, 163 (1999).
[4] T. Stoica, L. Vescan, and M. Goryll, J. Appl. Phys. **83**, 3367 (1998).
[5] A. Vonsovici, L. Vescan, R. Apetz, A. Koster, and K. Schmidt, IEEE Trans. Electron Devices **45**, 538 (1998).
[6] L. Vescan, C. Dieker, A. Hartmann, and A. van der Hart, Semicond. Sci. Technol. **9**, 387 (1994).
[7] L. Vescan, T. Stoica, O. Chretien, M. Goryll, E. Mateeva, and A. Mück, J. Appl. Phys. **87**, 7275 (2000).
[8] S. Luryi and E. Suhir, Appl. Phys. Lett. **49**, 140 (1986).
[9] D. B. Noble, J. L. Hoyt, C. A. King, and J. F. Gibbons, Appl. Phys. Lett. **59**, 51 (1986).
[10] B. W. Dodson, J. Cryst. Growth **111**, 376 (1991).
[11] T. Stoica and L. Vescan, J. Cryst. Growth **131**, 32 (1993).
[12] L. Vescan, T. Stoica, C. Dieker, and H. Lüth, Mater. Res. Soc. Symp. Proc. **298**, 45 (1993).
[13] S. Wickenhäuser, L. Vescan, K. Schmidt, and H. Lüth, Appl. Phys. Lett. **294**, 198 (1997).
[14] J. W. Matthewes and A. E. Blakeslee, J. Cryst. Growth **27**, 118 (1974).
[15] H. P. Tang, L. Vescan, C. Dieker, K. Schmidt, H. Lüth, and H. D. Li, J. Cryst. Growth **125**, 301 (1992).
[16] L. Vescan, R. Loo, C. Dieker, S. Wickenhäuser, A. Hartmann, and R. Apetz, Proceedings of the 24th ESSDERC Conference 1994, edited by C. Hill and P. Ashburn (Editions Frontieres, Gif sur Yvette, France, 1994), p. 749.
[17] R. Sauer, J. Weber, J. Stolz, E. R. Weber, K.-H. Küsters, and H. Alexander, Appl. Rev. A **36**, 1 (1985).
[18] A. Hartmann, L. Vescan, C. Dieker, T. Stoica, and H. Lüth, Phys. Rev. B **48**, 18276 (1993).
[19] D. W. Winston, SIMWINDOWS32 semiconductor device simulator v.1.5.0, Optoelectronics Computing Systems Center, University of Colorado, 1994.
[20] P. T. Landsberg, *Recombination in Semiconductors* (Cambridge University Press, Cambridge, 1991), pp. 346–352.
[21] D. V. Lang, R. People, J. C. Bean, and A. M. Segent, Appl. Phys. Lett. **47**, 1333 (1985).
[22] C. G. Van de Walle, Phys. Rev. B **39**, 1871 (1989).
[23] J. Weber and M. I. Alonso, Phys. Rev. B **40**, 5683 (1989).
[24] D. Dutartre, G. Bremound, A. Souifi, and T. Benyattou, Phys. Rev. B **44**, 11525 (1991).
[25] D. J. Robbins, L. T. Canham, A. D. Pitt, and P. Calcott, J. Appl. Phys. **71**, 1407 (1992).
[26] T. Stoica and L. Vescan, Presented at the E-MRS Conference-Strasbourg, Physica E (in press).
[27] *Silicon Germanium and SiGe:Carbon*, EMIS Data Reviews Series No. 24, edited by E. Kasper and K. Lyutovich (INSPEC, The Institution of Electrical Engineers, London, UK 2000).
[28] *Handbook Series on Semiconductor Parameters*, edited by M. Levinshtein, S. Rumyantsev, M. Shur, and Y. A. Pokrovskii (World Scientific, Singapore, 1996), Vol. 1, Chap. 1.